Supplementary Fig. 1: Astrocyte response to combination of TNF-α and IFN-γ.

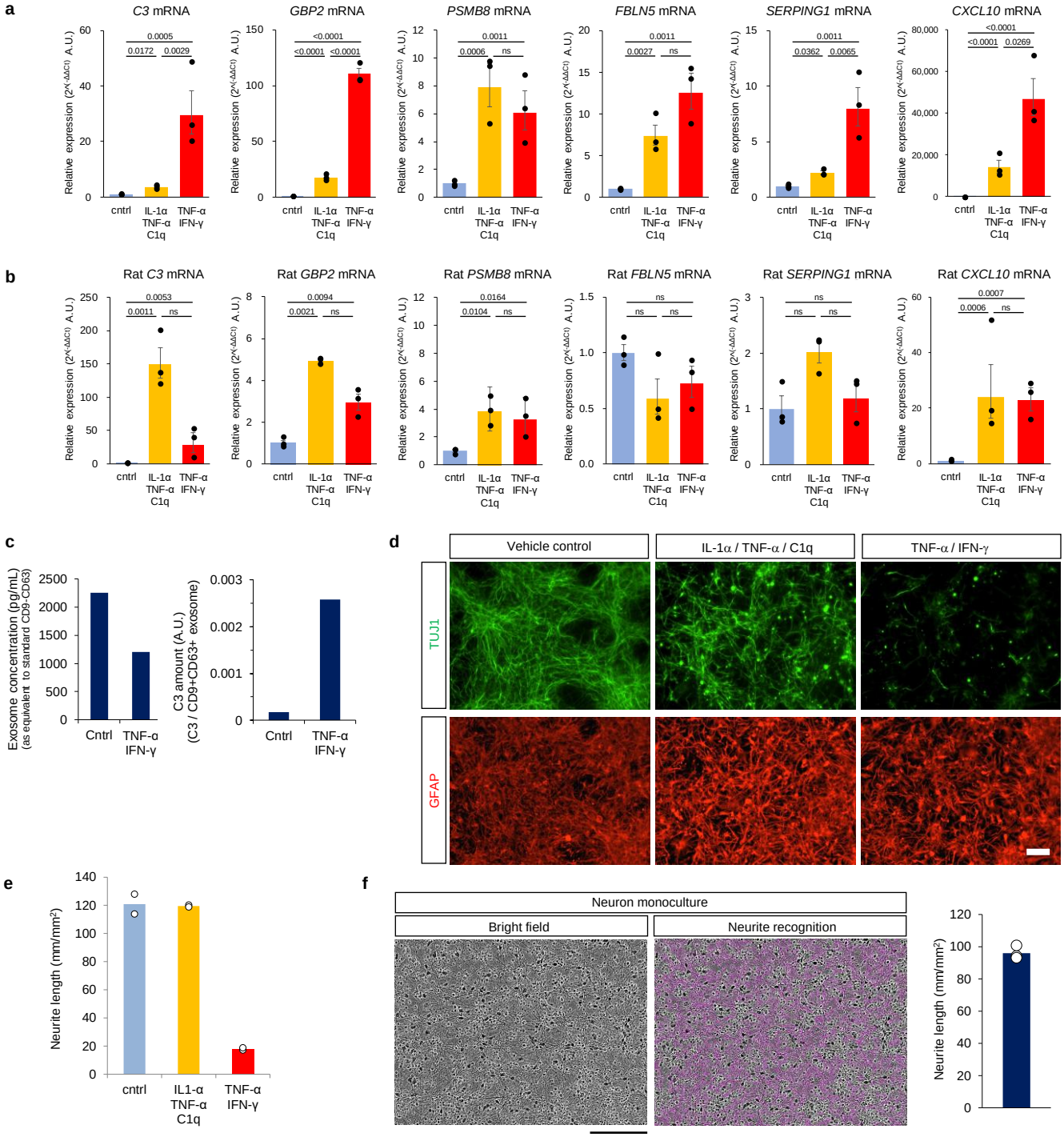

a-b, Relative gene expression levels of *C3*, *GBP2*, *PSMB8*, *FBLN5*, *SERPING1*, and *CXCL10* using *GAPDH* as the internal control in human iPSC-derived astrocytes (**a**) and rat primary astrocytes (**b**) cultured in serum-free rat astrocyte medium. Bar data represent mean ± s.e.m.; each dot represents an individual biological replicate ($n = 3$ independently prepared cells). Statistical analysis was performed using two-way ANOVA followed by Tukey's multiple comparisons test; ns: $P > 0.05$. **c**, Quantification of exosome concentration and C3 levels in exosomes isolated from the culture medium of human iPSC-derived astrocytes in the absence or presence of TNF-α and IFN-γ. **d-e,** Independent repeat experiment confirming stronger neurotoxicity induced by TNF-α and IFN-γ than by IL-1α/ TNF-α/C1q in human iPSC-derived astrocytes. Average neurite length from two technical replicate wells is shown in the bar graph (e). **f,** Bright-field image of NGN2-induced neuron monoculture maintained in differentiation medium and representative neurite recognition analysis. Neurites recognized by the Incucyte system are highlighted in magenta. Average neurite length from three technical replicate wells is shown in the bar graph. Scale bar: 100 µm (d), 200 µm (f)

Supplementary Fig. 2: Neurotoxicity assay and compound treatment.

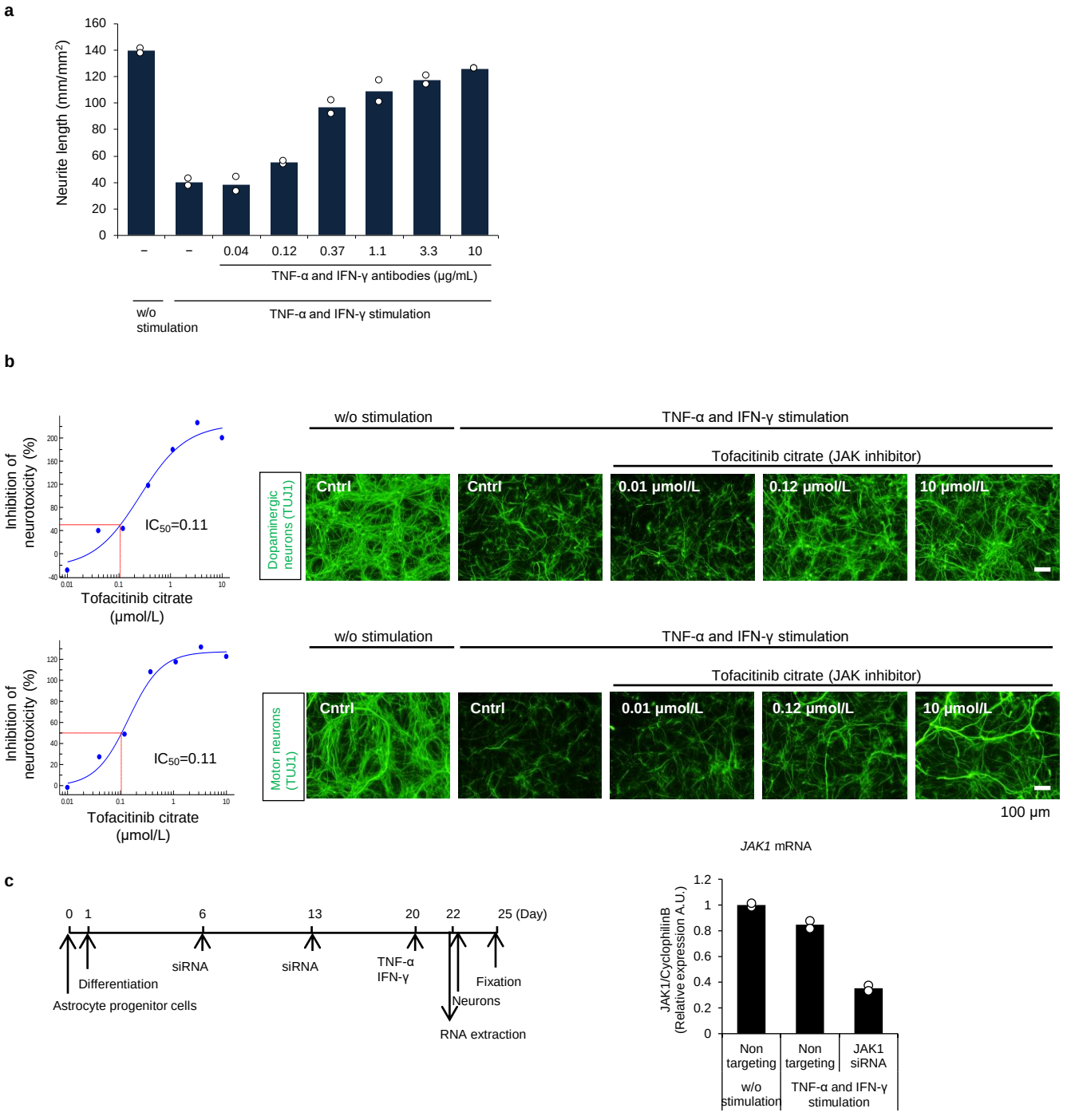

a, Neurite length was analyzed by measuring TUJ1-positive neurites of neurons cultured on human iPSC-derived astrocytes. The astrocytes were treated with TNF-α and IFN-γ in the presence or absence of neutralizing antibodies alongside TNF-α and IFN-γ. Bar data represent the average of two wells. Each dot represents an individual technical replicate (n = 2 wells). **b**, Neurotoxicity assay of astrocytes treated with Tofacitinib citrate using dopaminergic neurons and motor neurons. The dose-responsive curve is presented as the mean of n = 2 technical replicates. **c**, Schematic of gene knockdown using siRNA and confirmation of knockdown efficiency by qRT-PCR for *JAK1* mRNA. Bar graphs represent the average of 2 wells, and each dot represents an individual technical replicate (n = 2 wells).

Supplementary Fig. 3: Astrocyte progenitor culture duration and induction of *CDKN2A*.

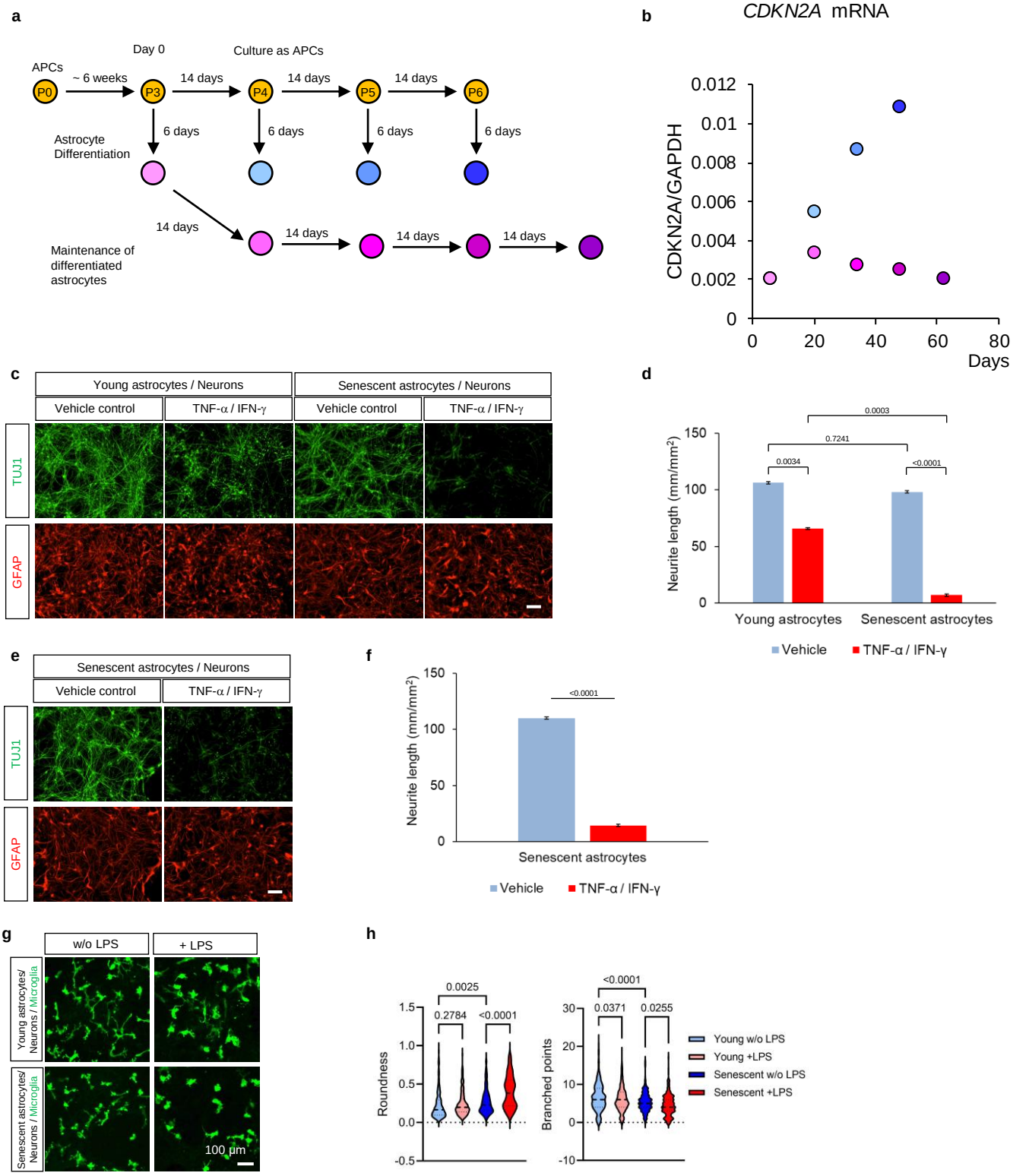

a, Schematic of culture of astrocyte progenitor cells (APCs), differentiation into astrocytes, and maintenance as astrocytes. Passage numbers at the APC stage are indicated. **b**, Relative levels of *CDKN2A* normalized to *GAPDH* mRNA quantified by digital PCR in astrocytes differentiated after different durations of culture as APCs (blue series of dots), or maintained as astrocytes (pink series of dots).

Supplementary Fig. 3: Astrocyte progenitor culture duration and induction of *CDKN2A*. (continued)

Data were obtained using XCell Science astrocyte progenitor cells (cat. no. XCS-AP-001-1V). Based on the senescence-associated increase in CDKN2A expression, astrocytes differentiated from P3 and P6 APCs were designated as young and senescent astrocytes, respectively. Representative images of TNF-α- and IFN-γ-induced neurotoxicity in these cells are shown in Fig. 4c. **c,** Representative images of TNF-α- and IFN-γ-induced neurotoxicity in astrocytes differentiated from P3 and P6 APCs from Applied StemCell (cat. no. ASE-9322P), which were designated as young and senescent astrocytes, respectively, based on the CDKN2A expression shown in Fig. 4b. **d,** Quantification of TUJ1+ neurite length in the co-cultures shown in (c). Bars indicate mean ± s.d. (n = 3 wells Statistical analysis was conducted using two-way ANOVA followed by Tukey's multiple comparisons test. **e,** Representative images of TNF-α- and IFN-γ-induced neurotoxicity in astrocytes derived from P7 APCs from Axol Bioscience (cat. no. AX0083), which were designated as senescent astrocytes based on the elevated CDKN2A expression shown in Fig. 4b. **f,** Quantification of TUJ1+ neurite length in the co-cultures shown in (e). Bars indicate mean ± s.d. (n = 3 wells). P values were computed using a two-sided t-test. **g,** IBA1 staining to visualize the morphology of microglia cultured on young or senescent astrocytes in the presence or absence of LPS. **h,** Roundness and number of branch points of microglia. Violin plots show median and quartiles for individual cells (n = 406 cells for young astrocytes w/o LPS, 347 cells for young astrocytes with LPS, 261 cells for senescent astrocytes w/o LPS, 220 cells for senescent astrocytes with LPS). Statistical analysis was conducted using one-way ANOVA followed by Tukey's multiple comparisons test. Scale bar: 100 μm

Supplementary Table 1：The source of the APCs and the passage number used for experiments

Figure	Origin of APCs	Passage number of APCs
Fig.1a	XCell Science	P6
Fig.1b	Axol Bioscience	P1
Fig.1c	XCell Science	P6
Fig.1f	Axol Bioscience	P6
Fig.1g	Axol Bioscience	P6
Fig.1j	XCell Science	P6
Fig.2c	Axol Bioscience	P7
Fig.2d	Axol Bioscience	P6
	Axol Bioscience	P6
	XCell Science	P6
Fig.2e	Axol Bioscience	P6
Fig.3ab	XCell Science	P6
Fig.3c	XCell Science	P6
Fig.4a	Applied StemCell	P3, P6
Fig.4b	XCell Science	P3
	Applied StemCell	P3
	XCell Science	P6
	Axol Bioscience	P7
	Applied StemCell	P6
Fig.4cd	XCell Science	P3, P6
Supplementary Fig.1a	XCell Science	P6
Supplementary Fig.1c	Axol Bioscience	P8
Supplementary Fig.1de	Axol Bioscience	P8
Supplementary Fig.2a	Axol Bioscience	P7
Supplementary Fig.2b	Axol Bioscience	P6
Supplementary Fig.2c	Axol Bioscience	P6
Supplementary Fig.3ab	XCell Science	P3, P4, P5, P6
Supplementary Fig.3cd	Applied StemCell	P3, P6
Supplementary Fig.3ef	Axol Bioscience	P7
Supplementary Fig.3gh	Applied StemCell	P3, P6

Supplementary Methods

EVs extraction and ELISA

Culture supernatants were collected from astrocytes treated with 7.5 ng/mL TNF-α and 5 ng/mL IFN-γ, or from vehicle-treated astrocytes. Exosomes were isolated from these supernatants using the MagCapture Exosome Isolation Kit PS (Fujifilm Wako) according to the manufacturer's protocol. The quantity of EVs was quantified using the CD9/CD63 Exosome ELISA Kit (Cosmo Bio). Briefly, a calibration curve was generated using a CD9/CD63 fusion protein as the standard, and the relative quantity of EVs in the samples was determined based on this standard curve. The amount of complement C3 in the EV samples was quantified using the Complement C3 Human ELISA Kit (Abcam). To evaluate the C3 content per EV, the total C3 concentration was normalized to the relative EV quantity in each sample.

Imaging analysis of microglial morphology

Image analysis was performed on two-channel micrographs comprising a nuclear staining channel and an IBA1 channel that selectively labels microglia. All computations were executed in Python 3.7.9; semantic segmentation networks were implemented in Keras (TensorFlow backend) and the thinning routine relied on the skeletonize function of scikit-image. Nuclear objects were first identified with a UNet-based model that assigns every pixel to one of three classes—nucleus, nuclear center or background—thereby providing both binary nuclear masks and discrete nuclear-center coordinates in a single forward pass. The microglial channel was independently processed with a second UNet that classifies pixels as soma, microglial processes or background. Both networks had been trained in advance on image sets acquired independently of the material analyzed here.

The preliminary soma mask was cross-checked against the nuclear mask. Any soma label devoid of an underlying nuclear signal was re-classified as microglial process, effectively eliminating false-positive somas. The validated soma and process regions were then skeletonized; branch points and termini of the resulting one-pixel-wide skeleton were regarded as graph nodes and the intervening skeletal segments as edges, yielding an undirected spatial graph for each microglial cell.

Nodes and edges located inside the soma were subsequently removed, and each soma was re-inserted into the graph as a single node positioned at its nuclear center. If a graph contained more than one nuclear-center node, neighboring microglia were considered to have been merged erroneously; in such cases, the graph was partitioned by severing the shortest path between individual nuclear centers until each sub-graph contained exactly one nucleus. For every cell-specific graph thus obtained, quantitative descriptors were extracted: the geometry of microglial processes (number of branch points, and related metrics).